AIAA JOURNAL
Vol. 34, No. 11, November 1996

Computational and Experimental Investigations of Rarefied Flows in Small Nozzles

Iain D. Boyd* and Douglas B. VanGilder†
Cornell University, Ithaca, New York 14853-7501
and
Edward J. Beiting‡
The Aerospace Corporation, Los Angeles, California 90009

Detailed numerical and experimental studies are presented for unheated flows of hydrogen and nitrogen through a small nozzle. The nozzle geometry and flow conditions considered provide rarefied flows that are representative of resistojet thrusters employed on spacecraft for control. Computational results are obtained with the direct simulation Monte Carlo method. Experimental data are obtained using two different techniques. Measurements of axial velocity and translational temperature of hydrogen are performed using coherent anti-Stokes Raman scattering. Data are taken along the nozzle axis and in the exit plane of the nozzle. Measurements of thrust are obtained using a thrust stand for pure hydrogen, pure nitrogen, and for mixtures of the two. In all cases, the numerical predictions and experimental measurements are in excellent agreement.

Introduction

THE useful life of a satellite is often limited by the amount of propellant carried onboard for station keeping or drag makeup. Thrusters with higher specific impulse make more effective use of the available fuel and extend the life of these satellites. A variety of electric propulsion devices are being developed that offer substantial improvements in performance over conventional chemical propulsion. Of the various electric propulsion devices, the resistojet[1] is the simplest. In this thruster, a gas flows over a resistively heated element, which imparts energy to the gas. This energy is converted to thrust by rapid expansion through a converging-diverging nozzle. Resistojets have been under development for many years and have been used in approximately 40 commercial spacecraft since 1980. Recent developments include the replacement of hydrazine monopropellant chemical thrusters by resistojets, which is expected to extend the life of satellites by more than 40%, resulting in a significant reduction in life cycle costs. As a step toward their wider use, a comprehensive understanding of this flowfield is required for performance improvement, spacecraft integration, and the provision of a basis for anomaly resolution. Review of the technical literature revealed that no comprehensive understanding of the flowfield is available. In particular, a theoretical model of the plume that can relate design modifications and operational changes to performance or spacecraft interaction with the plume is lacking.

Standard Navier–Stokes calculations have been shown to be inaccurate in describing resistojet flowfields.[2] The small geometric sizes (e.g., throat diameter less than 1 mm) and low flow rates (e.g., $\dot{m}$ of 10 mg/s) characteristic of resistojets yield Knudsen numbers at the nozzle exit that are so large that the assumptions invoked in applying the Navier–Stokes equations are invalidated. Shock tube studies have shown that the direct simulation Monte Carlo (DSMC) technique[3] offers better correspondence to experimental data under conditions where the Navier–Stokes equations break down. Initial experimental and theoretical studies of low-density supersonic jets of nitrogen and hydrogen have confirmed this conclusion.[2,4] The DSMC solutions, however, are quite sensitive to the models employed to simulate the interaction between molecules and the interaction between the gas and the nozzle wall surface. Thus wider application of this technique to rarefied flows (and in particular to resistojets) requires more detailed experimental measurements to anchor the calculations. The method has been applied to other low Reynolds number flows and is described in detail elsewhere.[2,4–6]

To extend the available database of these low-density-flows, Beiting[7] developed a diagnostic system to map velocity and translational temperature of the exhaust both inside and outside the nozzle of an operating resistojet. This diagnostic uses a nonlinear optical technique called coherent anti-Stokes Raman scattering (CARS). An optical technique is preferred because it does not perturb the flowfield, leaving the parameters undergoing measurement unchanged. The CARS technique allows a species to be probed with sufficient spatial resolution to generate maps that are useful for comparison with Monte Carlo calculations. Furthermore, it is applicable to the chemical species that are the main momentum carriers of the thrust in a hydrazine resistojet (H_2, N_2, and NH_3). This applicability allows questions such as the degree of velocity and temperature slippage among the momentum carriers to be studied; these topics cannot be addressed by techniques that probe seeded or minor species.

The organization of the paper is as follows. The resistojet and flow conditions employed in the present study are first described. Then a brief description of the DSMC code is provided. The experimental facility developed for this work is presented. The characteristics of the CARS technique for determination of velocity and translational temperature of molecular hydrogen is described. This is followed by a discussion of the experimental procedure. In the results section, separate discussions are provided on the comparisons of simulation and measurements for axial velocity, translational temperature, and specific impulse. The paper ends with a short summary.

Resistojet Simulator

The apparatus used to create a simulated resistojet flowfield is shown in Fig. 1. It was built by the NASA Lewis Research Center and is an improved version of configuration 2 used in Ref. 2. It comprises a 250-W (max.) heat exchanger, a plenum chamber, and a nozzle. Table 1 gives the flow rates, vacuum tank pressure, and diagnostics applied for all of the cases considered. For the results presented here, the plenum temperature is room temperature (293 K). The flow rates are measured using mass flow meters, which are calibrated by a volume displacement technique. Pressure readings at the inlet (marked "gas in" in Fig. 1) and in the plenum (marked "pressure tap" in Fig. 1) are taken with mechanical (Bourdon type) gauges with an accuracy of ±250 Pa. The inlet pressures to the system are about 3000 Pa higher than the plenum pressures for

Received March 25, 1996; revision received July 18, 1996; accepted for publication July 22, 1996; also published in *AIAA Journal on Disc*, Volume 2, Number 1.

*Associate Professor, School of Mechanical and Aerospace Engineering. Member AIAA.
†Graduate Research Assistant, School of Mechanical and Aerospace Engineering.
‡Research Scientist, Mechanics and Materials Technology Center. Member AIAA.

Table 1 Resistojet operating conditions

H_2:N_2, mg/s	CARS	Thrust	Tank pressure, mtorr
3.3:0.0	Yes	No	90
6.9:0.0	Yes	No	135
3.3:83.0	Yes	No	127
7.9–18.4:0.0	No	Yes	0.62–2.37
0.0:20.8–83.4	No	Yes	0.27–1.06
3.05:30.0	No	Yes	0.70
6.08:59.9	No	Yes	1.60

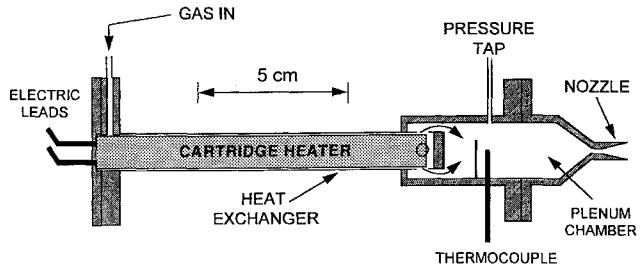

Fig. 1 Schematic diagram of the resistojet.

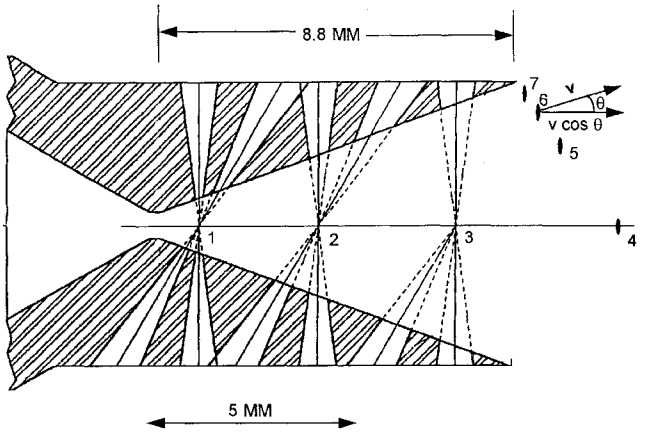

Fig. 2 Cross-sectional view of the ported nozzle.

the pure hydrogen flows. The chamber pressure is measured using a convectron (Granville Philips) gauge with an accuracy of ±0.25 Pa.

The DSMC simulations begin at a location just downstream of the nozzle throat. Initial flow conditions are specified using isentropic theory, the stagnation temperature, and the mass flow rate. The calculations proceed from the inlet plane out beyond the nozzle exit plane into the near-field plume expansion. This allows direct comparison with some of the experimental measurements that are taken a short distance into the plume from the nozzle exit. The expansion process is assumed to occur into the finite chamber pressure measured experimentally.

The nozzle dimensions are given in Table 2. Two versions of this nozzle are used for these studies: a ported nozzle for interior and exterior CARS measurements and a solid nozzle for exterior CARS measurements and thrust measurements. A microscopic examination of the nozzle throats indicates the throat area of the ported nozzle is about 10% larger than the solid nozzle area and about 13% greater than the specified area. To a certain extent, this discrepancy is reflected in the measured value of plenum pressure, which is found to be 20% lower for the ported nozzle. However, since the pressure is set by the mass flow rate, it is expected that the pressure will scale linearly with the area of the throat. Thus, the measured difference between the plenum pressures of the solid and ported nozzles is too large to be attributed solely to the 10% difference in throat areas. It is speculated that the additional drop in pressure is due to gas flow through the conical ports.

Figure 2 shows the series of conical holes cut in the side of the ported nozzle. Two pairs of holes are needed for the passage of the converging-diverging laser beams at the two angles required to make a velocity measurement (position 3 does not require an exit hole for the 30-deg measurement angle because the beams exit beyond the end of the nozzle). The 15-deg apex angle of the cone is dictated by the convergence angle of the laser beams. The conical shape of the holes is required to reduce the effect of the holes. Table 3 lists the values of the ratio of the sum of the breakthrough area of the holes to the cross-sectional area of the nozzle at the measurement point. In all cases, these values are less than 0.08.

Table 2 Nozzle dimensions (in millimeters)

Parameter	Specified	Solid	Ported
Inlet diameter	15.75	——	——
Throat diameter	0.66 ±0.005	0.67 ±0.005	0.70 ——
Inlet half-angle, deg	30	——	——
Exit half-angle, deg	20	——	——
Aero ratio	114	111	102

Table 3 Ported nozzle specifications

Position no.	Axial distance from throat, mm	Nozzle cross-sectional area, mm^2	Ratio of total ported area to nozzle cross-sectional area
1	0.96	1.51	0.075
2	3.84	9.80	0.076
3	7.20	28.36	0.045
4	11.10	——	——

Numerical Technique

A computer program based on the DSMC[3] method for application to electric propulsion is under development at Cornell University. The DSMC technique models gas flow at the molecular level using particles, the coordinates and properties of which are stored in the computer. The motion of particles is decoupled from collisions over a time step that is shorter than the mean time between collisions. The particles move through physical space according to their velocity components. Collisions are computed statistically using concepts from kinetic theory. A computational grid is employed to group together particles that are most likely to collide and to output flowfield data. The DSMC code used in this study[4] is implemented efficiently on a Cray C90 computer and has been verified directly against experimental data for flows in small thrusters of nitrogen, hydrogen, and helium.[2,4,6]

Elastic collisions are modeled with the variable hard sphere model[3] using parameters employed in Refs. 8 and 4 for nitrogen and hydrogen, respectively. In simulating the mixture of hydrogen and nitrogen, the modeling of rotational relaxation requires particular attention. The rate of rotational relaxation for hydrogen is at least one order of magnitude slower than for molecular nitrogen. Separate relaxation models are employed that have been previously developed and verified for nitrogen[8] and hydrogen.[4] The interaction between the particles and the nozzle wall uses diffuse reflection with full accommodation of energy to the nozzle wall temperature, which is assumed to be 293 K in all of the computations reported here.

The simulations employ up to 40,000 cells and a total of 5,00,000 particles. Total execution time on a Cray C90 supercomputer is quite long due to the relatively high density. The Knudsen number at the throat of the nozzle is about 5×10^{-4}. Although the Knudsen number increases by two orders of magnitude as the gas expands to the nozzle exit, most of the flow remains in the continuum flow regime. In this case, the total time required to obtain the DSMC solution is about 7 h.

Experimental Investigation

Test Facility

The test chamber is shown in Fig. 3. A 1.1-m-long × 0.75-m-diam stainless steel chamber is evacuated with two root pumps in parallel. The conductance of the 35 m of pipe between the pumps and chamber reduces the effective pumping speed at the chamber to between 100 and 500 l/s, depending on the gas composition and

pressure. At the chamber, the pipe is divided into two branches. One branch evacuated the chamber through two large diffusion pump ports (not operating for this work) located at the base of the chamber; the other branch evacuates a 10-cm-diam port that is directly in line with the exhaust of the jet when it is in the 0-deg position. The position of this port has a marked effect on the tank pressure when operated at high mass flow rates and the exhaust is forward directed into this port (see column 4 of Table 1). The base pressure of the system (no flow through the jet) is 0.4 Pa. The jet is mounted on a motorized $x-y$ stage that permitted positioning the jet along the flow axis and in a vertical plane. This assembly rests on a motorized stage that permits rotation of the jet around the measurement point (focal point of the laser beams) in the horizontal plane. The flow and laser beams are confined to the horizontal plane. The motion is computer controlled from outside the evacuated chamber.

CARS Diagnostic

A detailed discussion of the CARS technique applied to the resistojet was presented previously and the method is only briefly discussed here.[7] CARS is a four-wave mixing process in which a pump beam at angular frequency ω_p and a Stokes beam at ω_s interact through the third-order susceptibility of a medium, $\chi^{(3)}_{\mathrm{CARS}}$ to create a new beam at anti-Stokes frequency ω_{as}. When the difference frequency between the two input beams equals a resonance in the (hydrogen) medium, the strength of the anti-Stokes signal, which exits as a collimated beam, becomes large. If the input beams are monochromatic and phase matched (aligned so that photon momentum is conserved), the essentials of the CARS process can be understood from a simple expression for the signal intensity[9]

$$I_{as} = \left[\frac{16\pi^2\omega_{as}}{c^2}\right]^2 |\chi^{(3)}_{\mathrm{CARS}}|^2 I_p^2 I_s \lambda^2 \qquad (1)$$

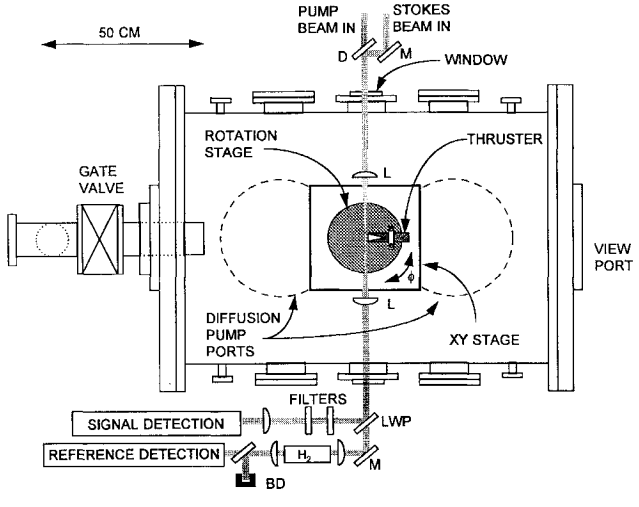

Fig. 3 Test chamber used for the CARS measurements.

where c is the speed of light and I_p and I_s are the intensities of the pump and Stokes beams, respectively. In a low-pressure gaseous medium, phase matching can be achieved by collinearly aligning the input beams. Using this geometry here, good spatial resolution is attained by tightly focusing the input beams (since the signal intensity depends on the cube of these intensities) and λ is the distance over which the beams coherently interact. For the tightly focused, collinearly aligned beam geometry used in this work, λ is the distance over which most of the CARS signal is generated, i.e., the spatial resolution. For molecules with no excited vibrational modes, the susceptibility scales linearly with the number density of the ground state of the resonance being probed. Accordingly, CARS measurements in low-density high-temperature flows are signal strength limited inasmuch as the signal decreases quadratically with this number density. Equation (1) also indicates that there is a direct tradeoff between the spatial resolution and signal strength because the signal strength also scales as λ^2. At the temperatures encountered in this work, nearly all of the hydrogen is in the $J = 1$ rotational level and only the $Q(1)$ resonance is used to obtain the velocity and temperature information.

The molecular resonances are also embodied in the susceptibility factor. For hydrogen at the low densities considered here, these are nonoverlapping resonances whose linewidths are a function of the temperature-dependent widths. The temperatures are extracted from these widths. If the gaseous medium has a flow velocity, the frequency of the resonance is shifted by the Doppler effect. This Doppler shift is used to infer the velocity of the flow. Two scans are used to measure the velocity at a single point. The first (reference) scan is taken with the laser beams perpendicular to the axis of the thruster (generating zero frequency shift) and the second with the beams at 60 deg with the axis. The spectral position of the $Q(1)$ line at the two angles is compared and the gas velocity is inferred from the frequency shift.

A block diagram CARS instrument is shown in Fig. 4. The second harmonic output of a commercially available single longitudinal mode (SLM) Nd:YAG laser provides the pump radiation for the CARS process as well as the excitation radiation for the dye laser system. The scanning SLM dye laser produces the tunable narrowband Stokes radiation required to scan across the $Q(1)$ Raman transition. This dye laser was built in-house because no comparable system is commercially available. Its performance defines the accuracy with which the velocity and temperature measurements can be made.

A small fraction of the Stokes beam is directed through an etalon to monitor the laser scan rate by creating a series of etalon peaks spaced at 1-GHz intervals. Then the Stokes and pump radiation are combined by a dichroic mirror and the collinear beams are directed through a wall into an adjacent laboratory where the thruster test facility resides. Inside a chamber that houses the thruster, the beams are tightly focused by a lens into the flowfield where the CARS signal is created. This tight focusing results in a spatial resolution measured to be better than 30 μm in the axial direction and 300 μm in the radial direction of the flow. The signal, pump, and Stokes beams are recollimated with a second lens before exiting the chamber. The signal is then separated from the laser beams with a dichroic

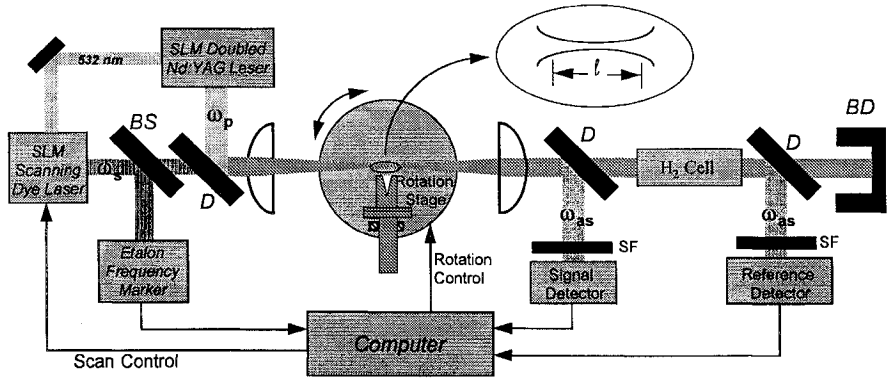

Fig. 4 Principal components of the CARS instrument used to measure velocity and translational temperature: BS = beam splitter, D = dichroic mirror, SLM = single longitudinal mode, and SF = spectral filter.

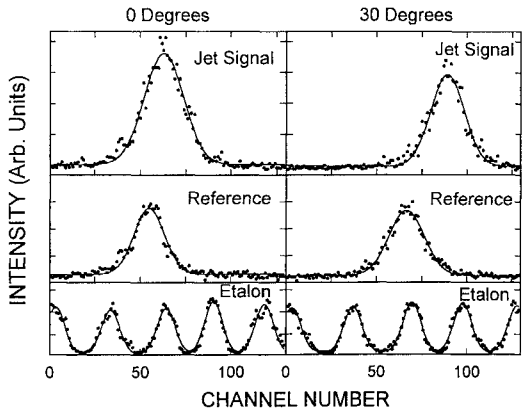

Fig. 5 Gaussian fits to the CARS data taken in the jet, in the reference cell, and to the etalon traces. These signal spectra were taken at position 2 shown in Fig. 2 with a plenum gas temperature of 294 K.

mirror and routed through several spectral filters before detected by a photomultiplier whose output is digitized and sent to a computer. On a parallel path, the separated pump and Stokes beams are focused into a cell filled with hydrogen creating a reference frequency from its $Q(1)$ line.

CARS Measurement Procedure and Data Reduction

After a stable flow and temperature in the jet are established, spectra of the $Q(1)$ line are taken. Figure 5 displays typical data from the measurement sequence required to recover one velocity and two linewidth (temperature) measurements at a single point in the gas flow. The signal, reference, and etalon traces displayed vertically are acquired simultaneously with a single scan of the dye laser; the 0- and 30-deg sets of spectra are taken sequentially. In general, the two sequences are taken automatically, the computer controlling the rotation of the stage from the 0- to the 30-deg position. However, an error in the machining of the two sets of holes for position 2 required adjusting the x–y translator between the measurements at the two angles. Thus, the 0- and 30-deg spectra are taken at slightly different locations in the gas flow at this position. Data from 10 laser pulses are averaged to create each of the 129 data points shown in each trace. The signal from each pulse is normalized by the pulse energy of the dye laser to account for shot-to-shot fluctuations of its output. Approximately 5 min are required to acquire the data shown in the figure. About half of this time is due to the acquisition of the data (1 s/point for the laser operating at 10 Hz) and half for processing the data and stepping the dye laser.

The data reduction is automated. Each of the peaks shown in Fig. 5 is fit to a Gaussian function where the center, width, height, and baseline are adjustable parameters. The difference between the channel number of the peak of the signal scan and that of the reference scan is converted to a frequency using the spacing of the peaks in the etalon trace. (Each peak in the etalon trace is separated by 1 GHz.) This frequency for the 0-deg scan is subtracted from the corresponding frequency for the 30-deg scan and the result is used to calculate the velocity as follows. For collinear phase matching, the Doppler shift of the anti-Stokes frequency $\Delta\nu_D$ for a flow velocity v is

$$\Delta\nu_D = \tilde{\nu}_R v \cos\alpha \tag{2}$$

where $\tilde{\nu}_R$ (cm^{-1}) is the Raman shift and α is the angle between the laser propagation and flow velocity.[7] For the hydrogen $Q(1)$ line ($\tilde{\nu}_R = 4155$ cm^{-1}) and for a 30-deg rotation angle, v (km/s) = $4.81\Delta\nu_D$ (GHz). Nonlinearities in the scanning mechanism of the Stokes laser limited the precision of the velocity measurements to about 0.2 km/s.

The channel width of the signal Gaussian was converted to a frequency width also using the values from the etalon peaks. This measured width is used to infer the translational temperature of the hydrogen using the following procedure. For monochromatic waves, the CARS resonance linewidth may be approximated as 1.23 times the Raman Doppler width for forward scattering, i.e.,

$$\Gamma = 2.46\frac{\omega_R}{c}\sqrt{\frac{2kT\,\ell n(2)}{m}} \tag{3}$$

where Γ is the full width half height, ω_R is the frequency of the Raman resonance, T is the absolute temperature, and m is the molecular mass. This approximation is good below 10 torr for hydrogen. For the $Q(1)$ transition of H_2, $\Gamma = 77.65$ MHz $\sqrt{(T)}$. In the absence of other broadening effects, the measured width is obtained from the convolution of the resonance line (Galatry) function with Gaussian line functions of the lasers. However, the low molecular densities encountered in the resistojet required using laser intensities that caused broadening of the resonance line by both stimulated Raman gain and the ac Stark effect. The broadening due to these effects is individually measured for this instrument using a line narrowed sample of hydrogen in a cell (77 K, 104 kPa). The functional dependence of the linewidth on both pump and Stokes laser intensities is measured and this empirical information is used to obtain the resonance width. The temperature is then inferred from this width using Eq. (3). Details of the procedure are presented in Ref. 7.

Thrust Measurements

The thrust measurements are made using an apparatus built at The Aerospace Corporation based on a design by NASA Lewis Research Center.[10] The thrust of the resistojet causes the displacement of a hinged platform against a spring of known force constant. The displacement is registered using a displacement-to-voltage transducer whose output is sampled by computer at 100 Hz and averaged to record a thrust level every second. The thrust balance is calibrated periodically during the measurements by shutting off the gas flow to the resistojet and recording the displacement of the platform caused by a series of four weights of known mass. The thrust balance is enclosed in a water-cooled copper box to thermally isolate it from the resistojet. A detailed description of this thrust stand and calibration method is available in Refs. 11 and 12.

For the present application, the calibration weights each have a mass of approximately 0.0054 kg. The four known masses are permitted to act on the thrust platform additively and then subtractively (0, 1, 2, 3, 4, 3, 2, 1, 0) for each calibration sequence, allowing a five-level calibration up to 211.58 mN. The calibration sequence creates nine data points that are fit to a straight line to obtain the force constant (mN/mV) and baseline. The R^2 values for all of the linear fits are >0.9999, indicating negligible nonlinearity. The force constants and baselines for the two calibration sequences before and after a series of measurements are averaged to produce the force constant and baseline used to infer thrust levels for the flow conditions investigated. This method leads to an uncertainty of ±0.5 mN in the thrust measurements. Measured thrust levels vary between 4 and 121 mN.

The thrust measurements are performed in a larger vacuum facility than that employed for the CARS investigation. In this case, a 5.5-m-long × 2.4-m-diam stainless steel chamber is evacuated by 14 diffusion pumps, which create a pumping speed of about 50,000 l/s for nitrogen and about twice that for hydrogen. This higher pumping capability allows the thrust measurements to be conducted at higher vacuum than for the CARS study. Flow rates are again measured using mass flow meters, which are calibrated using a volume displacement technique such that flow rates are measured to an accuracy of 1%. For the highest flow rate considered in this study (see Table 1) the background pressure in the test chamber is raised to 1.60 mtorr. Most measurements are taken at chamber pressures below 1.00 mtorr. Studies on the effect of chamber pressure on measured resistojet thrust[13] indicate that thrust is reduced (by about 7%) only at pressures greater than 10 mtorr at high temperatures due to convective heat losses. Thrust measurements of resistojets at room temperature remain unaffected by background pressure at levels as high as 1 torr.

Results

General features of the nozzle and near-field plume expansion region are shown in Fig. 6. This shows the DSMC solution for Mach

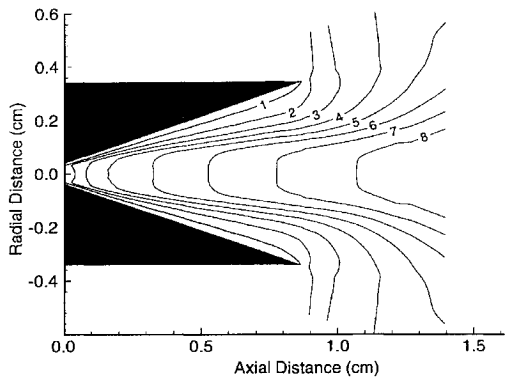

Fig. 6 Contours of Mach number predicted by the DSMC method for pure hydrogen flow with $\dot{m}$ = 6.9 mg/s.

number for the pure hydrogen flow in which the flow rate is 6.9 mg/s. It is found that a very thick viscous boundary layer develops under these flow conditions due to the relatively low throat Reynolds number of a few hundred. Also note that the flow is rapidly expanded to Mach numbers as high as 8 in the near-field expansion region. In the following, separate discussion is provided on comparisons of DSMC results and experimental data for 1) flowfield measurements of axial velocity, 2) flowfield measurements of translational temperature, and 3) performance measurements of specific impulse.

Axial Velocity

The velocity of molecular hydrogen is measured at three axial positions inside the nozzle and one axial and three off-axis positions outside the nozzle. The four points marked 1–4 in Fig. 2 are studied using the ported nozzle; the four points marked 4–7 are made with the solid nozzle. The redundant measurement at position 4 is used to compare the effect of the holes on the velocity.

Figures 7a and 7b present the velocities measured at points 1–4 for the first three cases listed in Table 1. Figures 8a and 8b present the velocities for these flow rates for the exterior points taken using the solid nozzle. Each datum point is an average of three to six measurements. The error bars are the standard deviations and not the accuracy of the measurements, which is limited to 0.2 km/s by the linearity of the dye laser drive. The DSMC calculations are shown by the solid lines in these figures.

Consider the comparisons for the axial velocity of hydrogen shown in Fig. 7a for both of the pure hydrogen flows. The DSMC solution is that obtained at a flow rate of 6.9 mg/s. In terms of both axial velocity and translational temperature, this solution is almost identical to that obtained at a flow rate of 3.3 mg/s. In Fig. 7b, the comparison between measurement and prediction for velocity of hydrogen in the gas mixture case is shown. First note that, in all three cases, the two measurements obtained at location 4 for the ported and solid nozzles agree to within 10%, which is lower than the measurement uncertainty. This has the significance of indicating that there is no effect on the flows through the ported nozzle of the CARS access holes. It is found in all cases that the DSMC calculations of velocity agree very well with the measurements. Note the effect of introducing nitrogen flow on the flow velocity as shown in Fig. 7b. It is extremely satisfying to find that the DSMC predictions retain their accuracy in this gas mixture.

Figures 8a and 8b present the velocities at the exterior points where the solid nozzle is used. Once again, the single DSMC solution shown in Fig. 8a is that obtained at a flow rate of 6.9 mg/s. The data are plotted as a function of the angle subtended to the axis by a radius originating at the nozzle throat. In these cases, measurements and calculations are again in excellent agreement. The size of the boundary layer formed in each of the three flows may be estimated from the point where the velocity first begins to decrease away from the axis located at an angle of 0 deg. Thus, it is found that significant boundary-layer thicknesses of about 70% exist for the pure hydrogen flows, whereas the addition of nitrogen produces a much smaller boundary layer of about 20%. It is significant that the DSMC results provide such excellent agreement, indicating accurate simulation of

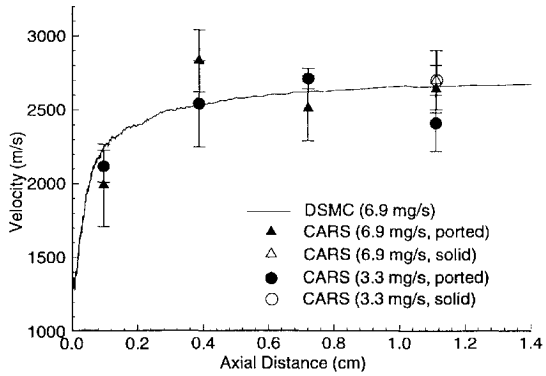

a) Pure hydrogen flows

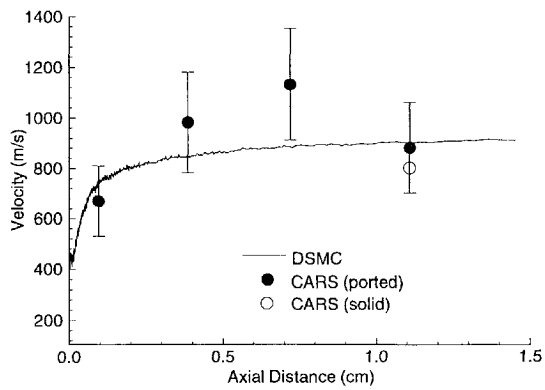

b) Mixture of hydrogen and nitrogen

Fig. 7 Hydrogen velocities at the interior of the resistojet nozzle.

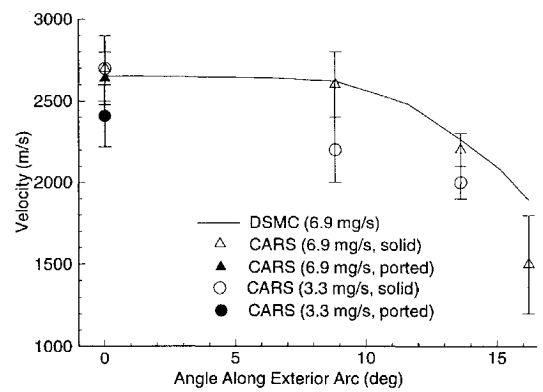

a) Pure hydrogen flows

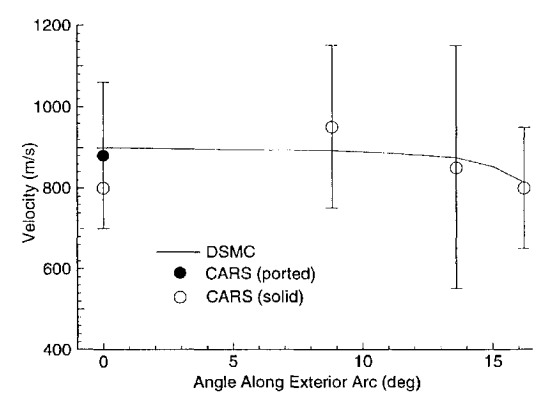

b) Mixture of hydrogen and nitrogen

Fig. 8 Hydrogen velocities at the exterior of the resistojet nozzle.

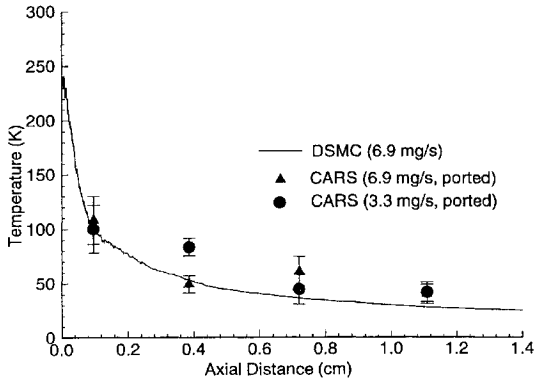

a) Pure hydrogen flows

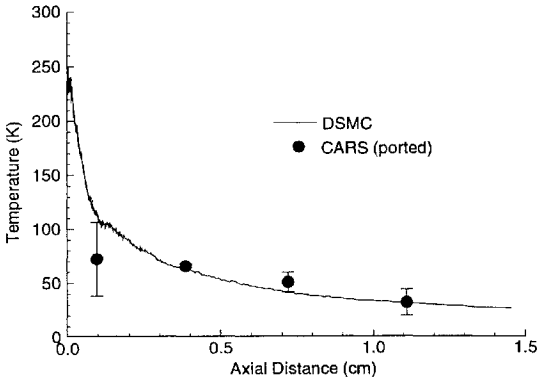

b) Mixture of hydrogen and nitrogen

Fig. 9 Hydrogen translational temperatures at the interior of the resistojet nozzle.

viscous effects. Precise computation of the boundary layer is a key component of predicting plume interaction effects since it is this region of the nozzle that contributes most to the backflow. Since every effort is made in spacecraft design to point the thruster away from spacecraft surfaces, it is in the backflow region that much of the interaction effects occur.

Translational Temperature

Figures 9a and 9b present measured and calculated values of the translational temperature of hydrogen for the first three flow conditions of Table 1. The two sets of measured data for pure hydrogen are compared with the DSMC result obtained at a mass flow rate of 6.9 mg/s in Fig. 9a. Reduction of the CARS measurements to translational temperatures is performed only for the flow along the axis due to lack of signal in the exterior measurement data. Once again, the error bars are the standard deviations of the four-to-eight measurements made at each position and should not be interpreted as the accuracy of the measurements. The corrections to the temperature due to the line broadening mechanisms mentioned earlier are on the order of 100 K (Ref. 7). The absolute accuracy of the temperatures are estimated to be about 30%. Given the uncertainty in the measurements, the agreement between the calculated and experimental values are considered very good in all three cases. These comparisons represent one of the first opportunities to assess translational temperature predictions of the DSMC technique. Previous comparisons have focused on pitot pressure[2] and rotational temperature.[4]

An interesting aspect of low-density flows is nonequilibrium effects such as thermal nonequilibrium and velocity slip between different species and different energy modes. These phenomena are simulated directly by the DSMC technique. It is found in the flow conditions investigated that the densities are sufficiently high to avoid any slip effects in either temperature or velocity.

Specific Impulse

As described previously, a number of measurements of thrust are conducted in pure hydrogen, in pure nitrogen, and in mixtures of the

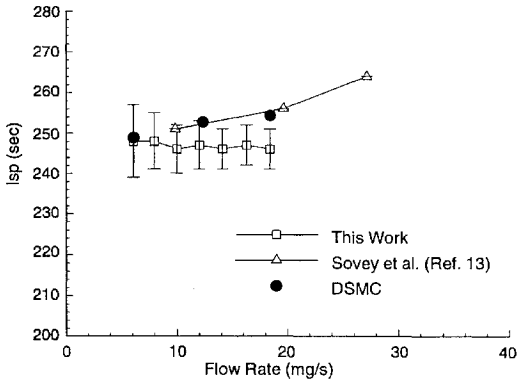

a) Pure hydrogen

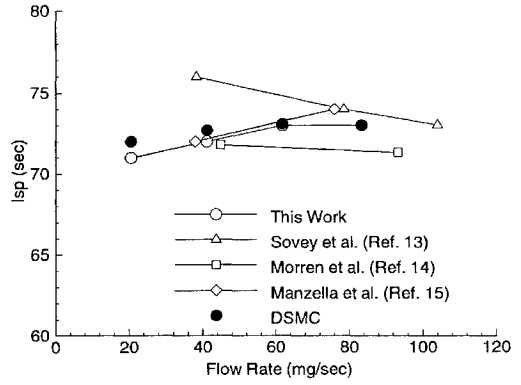

b) Pure nitrogen

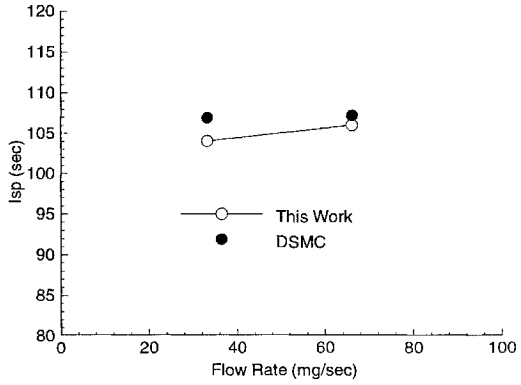

c) Mixture of 60% hydrogen and 40% nitrogen

Fig. 10 Specific impulse as a function of flow rate.

two. In each case, a range of flow rates is investigated. These data are compared with the results of corresponding DSMC simulations in Figs. 10a–10c.

In Fig. 10a, the data are shown for flows of pure hydrogen. Data taken from a previous experimental study by Sovey et al.[13] using a similar resistojet geometry are also included. The experimental data obtained in the present investigation offer reasonable agreement with the prior experimental investigation. The DSMC results show a very small increase of specific impulse with flow rate and appear to lie right in the middle of the two experimental data sets.

The data for flows of pure nitrogen are shown in Fig. 10b. Once again, data from previous experimental investigations[13–15] are included. The scatter in all of the experimental and numerical data is quite small, and it is clear that the DSMC technique is able to predict the performance of cold nitrogen thrusters with great accuracy.

The data for the mixtures of hydrogen and nitrogen are shown in Fig. 10c. No previous data for such mixtures appear in the literature. The agreement between prediction and measurement is again very good with the two lying within 5% of one another.

The comparisons between DSMC prediction and experimental measurement for resistojet performance shown in Figs. 10a–10c

are the first to appear in the literature. It is clearly significant that this numerical technique is able to predict specific impulse with such accuracy. In addition to implications for improved design and spacecraft integration of resistojets, the success reported here offers the potential that the DSMC technique can be developed for analysis of new electric propulsion devices such as arcjets and ion thrusters.

Summary and Concluding Remarks

Detailed experimental data have been obtained with the CARS technique for axial velocity and translational temperature of hydrogen in a gas mixture representative of flow in a hydrazine resistojet. These data were used to successfully validate the ability of the direct simulation Monte Carlo method to simulate these flows. The good agreement obtained with the detailed flowfield measurements indicates that the DSMC technique may be used with confidence to provide an accurate description of the expansion plume. Hence, the DSMC method is capable of providing an accurate estimate of plume impingement effects such as heating, torques, and contamination.

Comparison of numerical results with experimental measurement of thrust was also good. The DSMC technique consistently predicted specific impulse for pure hydrogen, pure nitrogen, and mixtures of hydrogen and nitrogen. These successful comparisons indicate that the DSMC technique may be used with confidence for design studies that aim to improve the performance of resistojets.

Thus, in the present extensive investigation, it has been established through direct comparison with experimental data that the DSMC method provides accurate simulation of the flowfields and performance characteristics of a cold flow resistojet. Further work is under way to consider heated flows.

Acknowledgments

Funding for the work at Cornell was provided by NASA Lewis Research Center under Grant NAG3-1451. The work at The Aerospace Corporation was supported by the U.S. Air Force Office of Scientific Research, the U.S. Air Force under Contract F04701-93-C-0094, and The Aerospace Corporation. Computer resources on the Cray C90 were provided by the National Aerodynamic Simulator at NASA Ames Research Center. The authors thank Frank Curran, Eric Pencil, and Donna Zelesnik of NASA Lewis Research Center for the resistojet, Lissa Garman for technical assistance in the laboratory during the development of the CARS instrument, and Richard Welle and James Pollard for assistance with the thrust measurements.

References

[1]Edwards, I., and Jansson, R. E. W., "Gasdynamics of Resistojets," *Journal of the British Interplanetary Society*, Vol. 24, 1971, pp. 729–742.

[2]Boyd, I. D., Penko, P. F., Meissner, D. L., and DeWitt, K. J., "Experimental and Numerical Investigations of Low-Density Nozzle and Plume Flows of Nitrogen," *AIAA Journal*, Vol. 30, No. 10, 1992, pp. 2453–2461.

[3]Bird, G. A., *Molecular Gas Dynamics and Direct Simulation of Gas Flows*, Oxford Univ. Press, Oxford, England, UK, 1994.

[4]Boyd, I. D., Beattie, D. R., and Cappelli, M. A., "Numerical and Experimental Investigations of Low-Density Supersonic Jets of Hydrogen," *Journal of Fluid Mechanics*, Vol. 280, 1994, pp. 41–67.

[5]Boyd, I. D., "Vectorization of a Monte Carlo Method for Nonequilibrium Gas Dynamics," *Journal of Computational Physics*, Vol. 96, 1991, pp. 411–427.

[6]Boyd, I. D., Jafry, Y. R., and Vanden Beukel, J., "Particle Simulations of Helium Microthruster Flows," *Journal of Spacecraft and Rockets*, Vol. 31, No. 2, 1994, pp. 271–277.

[7]Beiting, E. J., "CARS Measurements in Low Density Expanding Flows: Application to Resistojets," AIAA Paper 95-1962, June 1995.

[8]Boyd, I. D., "Temperature Dependence of Rotational Relaxation in Shock Waves of Nitrogen," *Journal of Fluid Mechanics*, Vol. 246, 1993, pp. 343–360.

[9]Nibler, J. W., and Pubanz, G. A., "Coherent Raman Spectroscopy of Gases," *Advances in Non-Linear Spectroscopy*, edited by R. J. H. Clark and R. E. Hester, Wiley, New York, 1988.

[10]Haag, T. W., and Curran, F. M., "Arcjet Starting Reliability: A Multistart Test on Hydrogen/Nitrogen Mixtures," AIAA Paper 87-1061, May 1987.

[11]Pollard, J. E., and Welle, R. P., "Thrust Vector Measurements with the T5 Ion Engine," AIAA Paper 92-2829, July 1995.

[12]Welle, R. P., Pollard, J. E., Janson, S. W., Crofton, M. W., and Cohen, R. B., "One Kilowatt Hydrogen and Helium Arcjet Performance," AIAA Paper 91-2229, July 1991.

[13]Sovey, J. S., Penko, P. F., Grisnik, S. P., and Whalen, M. V., "Vacuum Chamber Measurements Pressure Effects on Thrust Measurements of Low Reynolds Number Nozzles," *Journal of Propulsion and Power*, Vol. 2, No. 5, 1986, pp. 385–389.

[14]Morren, W. E., Hay, S. S., Haag, T. W., and Sovey, J. S., "Performance Characterizations of an Engineering Model Multipropellant Resistojet," *Journal of Propulsion and Power*, Vol. 5, No. 2, 1989, pp. 197–203.

[15]Manzella, D. H., Penko, P. F., DeWitt, K. J., and Keith, T. G., "Effect of Ambient Pressure on the Performance of a Resistojet," *Journal of Propulsion and Power*, Vol. 5, No. 4, 1989, pp. 452–456.